Md. Shuza Uddin*, Animesh Kumer Chakraborty, Stefan Spellerberg, Md. Asad Shariff, Sopan Das, Md. Abdur Rashid, Ingo Spahn, and Syed M. Qaim

Experimental determination of proton induced reaction cross sections on ^{nat}Ni near threshold energy

DOI 10.1515/ract-2015-2527
Received October 8, 2015; accepted November 17, 2015; published online January 22, 2016

Abstract: A newly developed facility at the 3 MV Tandem Accelerator at Dhaka for measurement of proton induced reaction cross sections in the energy region below 5 MeV is outlined and tests for the beam characterization are described. The results were validated by comparison with the well-known excitation function of the ^{64}Ni(p, n)^{64}Cu reaction. Excitation functions of the reactions ^{nat}Ni(p, x)^{60,61}Cu, ^{nat}Ni(p, x)$^{55,57,58m+g}$Co and ^{nat}Ni(p, x)^{57}Ni were also measured from threshold to 16 MeV using the stacked-foil technique, whereby irradiations were performed with 5 MeV protons available at the Tandem Accelerator and 16.7 MeV protons at the BC 1710 cyclotron at Jülich, Germany. The radioactivity was measured using HPGe γ-ray detectors. A few results are new, the others strengthen the database. In particular, the results of the reaction ^{nat}Ni(p, x)^{61}Cu below 3 MeV could serve as beam monitor.

Keywords: ^{nat}Ni target, cross sections, tandem accelerator, BC 1710 cyclotron, 5 MeV and 16.7 MeV protons.

***Corresponding author: Md. Shuza Uddin,** Tandem Accelerator Facilities, Institute of Nuclear Science and Technology, Atomic Energy Research Establishment, Savar, Dhaka, Bangladesh; and Institut für Neurowissenschaften und Medizin, INM-5: Nuklearchemie, Forschungszentrum Jülich, D-52425 Jülich, Germany, e-mail: md.shuzauddin@yahoo.com
Animesh Kumer Chakraborty: Tandem Accelerator Facilities, Institute of Nuclear Science and Technology, Atomic Energy Research Establishment, Savar, Dhaka, Bangladesh; and Department of Physics, Chittagong University of Engineering and Technology, Chittagong, Bangladesh
Md. Asad Shariff, Sopan Das: Tandem Accelerator Facilities, Institute of Nuclear Science and Technology, Atomic Energy Research Establishment, Savar, Dhaka, Bangladesh
Md. Abdur Rashid: Department of Physics, Chittagong University of Engineering and Technology, Chittagong, Bangladesh
Stefan Spellerberg, Ingo Spahn, Syed M. Qaim: Institut für Neurowissenschaften und Medizin, INM-5: Nuklearchemie, Forschungszentrum Jülich, D-52425 Jülich, Germany

1 Introduction

The use of low-energy charged particle accelerators ($E \leq 6$ MeV) in nuclear research is of considerable significance, with regard to both fundamental nuclear investigations and to application-oriented studies. Regarding fundamental studies, experimental investigation of nuclear reactions is quite interesting, especially near their thresholds, where the theoretically calculated results have fairly large uncertainties due to uncertainties in the estimation of the relative contributions of the three competing processes, viz. scattering, Coulomb excitation and deep penetration. Due to the expected low cross section of the latter process, clean experiments are needed for an unambiguous identification of the reaction product. The results obtained should shed some light on reaction mechanisms and the data could be useful for radionuclide production.

We chose to study proton induced nuclear reactions on nickel. It is an important element from practical point of view, being used as a construction material in nuclear technology and as a target material in accelerator production of medical radionuclides. In its natural composition it consists of five stable isotopes, namely ^{58}Ni (68.077%), ^{60}Ni (26.223%), ^{61}Ni (1.140%), ^{62}Ni (3.634%) and ^{64}Ni (0.926%). Cross section measurements on proton induced reactions have been done using all the five isotopes in highly enriched forms as targets (cf. [1–10]), mainly in the context of radionuclide production. In particular the non-standard positron emitters ^{55}Co ($T_{1/2}$ = 17.57 h), ^{61}Cu ($T_{1/2}$ = 3.33 h) and ^{64}Cu ($T_{1/2}$ = 12.7 h) are produced with high radionuclidic purity and in quantities sufficient for medical applications via the reactions ^{58}Ni(p, α)^{55}Co [9, 11], ^{61}Ni(p, n)^{61}Cu [6, 12] and ^{64}Ni(p, n)^{64}Cu [6, 8, 13–15], respectively. The measured excitation functions of those reactions have also been subjected to rigorous theoretical treatment (cf. [16–18]) and recommended sets of cross section data have been reported. As far as measurements on ^{nat}Ni are concerned, several groups reported data over various proton energy ranges (cf. [19–30]). In particular, Amjed et al. [22] reported extensive experimental data and performed a thorough analysis of all the data. The information

available is useful for validation of data measured using enriched target isotopes, for application in thin layer activation analysis, and for use in monitoring of proton flux during an irradiation. Many of those data were obtained via excitation function measurements using the stacked-foil technique with the incident proton energy on the first foil around 18 MeV or higher. The energy incident on each back foil of the stack was obtained by absorption calculations. Although in recent years adjustment of incident energies on back foils could be done using monitor foils rather successfully, it appears worthwhile to perform some measurements in the low-energy region (below 6 MeV) using a well-defined beam from a low-energy accelerator.

A 3 MV Tandem Accelerator (High Voltage Engineering Europa B.V.) was recently installed within the AERE Campus, Savar, Bangladesh. It delivers protons of energies < 6 MeV. So far it has been successfully used for analytical work, mainly using the particle induced X-ray emission (PIXE) technique [31]. Now it has been adapted to measure also nuclear reaction cross sections. In this paper we describe the irradiation facility, the characterization of the available beam and the validation of the measured data by comparison with the well-established excitation function of the ^{64}Ni(p, n)^{64}Cu reaction. Furthermore, several other excitation functions were measured from their thresholds up to 16 MeV proton energy using the cyclotron BC 1710 at the Forschungszentrum, Jülich, Germany. The results are compared with the literature experimental and theoretical data.

2 Experimental details

2.1 Measurements at 3 MV Tandem Accelerator

2.1.1 Irradiation chamber

A new experimental vacuum chamber was recently incorporated in the 3 MV Tandem Accelerator, installed within the campus of Atomic Energy Research Establishment, Savar, Dhaka. The set up for irradiation within the vacuum chamber is shown in Figure 1. The major function of the chamber is to allow use of standard ion beam analysis (IBA) techniques such as proton induced X-ray emission (PIXE), Rutherford backscattering spectrometry (RBS), etc. with millimeter-sized beam. To date the irradiation facility has been utilized for proton irradiations only. The chamber is 60 cm high and it has 39 cm diameter. It has 14 different size ports in it. The heart of the IBA chamber is a sample wheel with 25 holes, where samples can be mounted for irradiation. Just after the switching magnet and along the -30° exit port two pairs of variable beam slits are installed to define the beam profile for the IBA chamber, as necessary.

A beam profile monitor and a Faraday cup are also installed in the beam line to tune the beam before entering the experimental chamber. At the back of the chamber another wide and deep Faraday cup is installed to measure the beam current. The sample wheel is also connected to the current integrator in that Faraday cup. A voltage of −60 V is applied both at the entrance of the chamber and at the entry of the Faraday cup, whereas +60 V is applied at the sample wheel and the Faraday cup to suppress the secondary electrons.

Before irradiation the beam current was measured by the second Faraday cup. After reaching a constant value of 100 nA, the sample was moved to the proper position in the proton beam line and irradiated. During the irradiation the beam current was registered by charge collection.

2.1.2 Beam characterization

The energy of the extracted particle beam is given by the accelerator parameters. Special attention was paid to all three beam parameters, viz. shape, energy and intensity, which are very important in nuclear reaction cross section measurements. The beam shape was checked by the irradiation of a filter paper. A dark spot of about 5 mm diameter was observed which showed that the beam is focused and it is centric. The primary proton energy was checked by a comparison of activation products ^{63}Zn/^{65}Zn. The method involves a comparison of the normalized activities of two different threshold reaction products induced in a monitor foil [4, 32]. For this purpose a thin Cu foil (~ 10 μm thick) was placed in front of a target and irradiated with protons. The activities of the two products, viz. ^{63}Zn ($T_{1/2}$ = 38.47 min) and ^{65}Zn ($T_{1/2}$ = 244.93 d), were determined by γ-ray spectrometry using a high-resolution HPGe detector, and normalized for the cross section and the irradiation-time dependent saturation factor. Therefrom the ratio of the activities of ^{63}Zn/^{65}Zn was obtained. The ratio was also calculated theoretically from the IAEA recommended excitation functions of the two relevant reactions, namely ^{nat}Cu(p, x)^{63}Zn and ^{nat}Cu(p, x)^{65}Zn ([33], updated online version). From a comparison of the experimentally obtained and theoretically calculated ratio, the average energy of the proton beam within the first foil was deduced. A typical result is shown in Figure 2. The energy deduced in this way

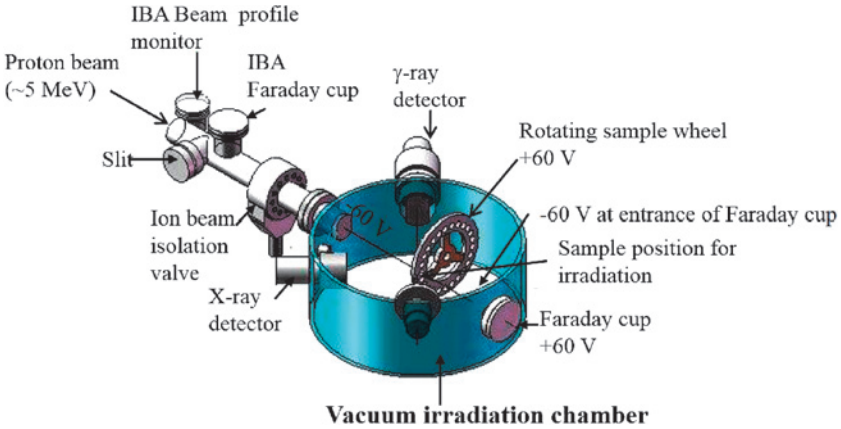

Figure 1: Schematic diagram of experimental setup at 3 MV Tandem Accelerator in Dhaka, adapted to irradiation of thin foils with low-energy protons.

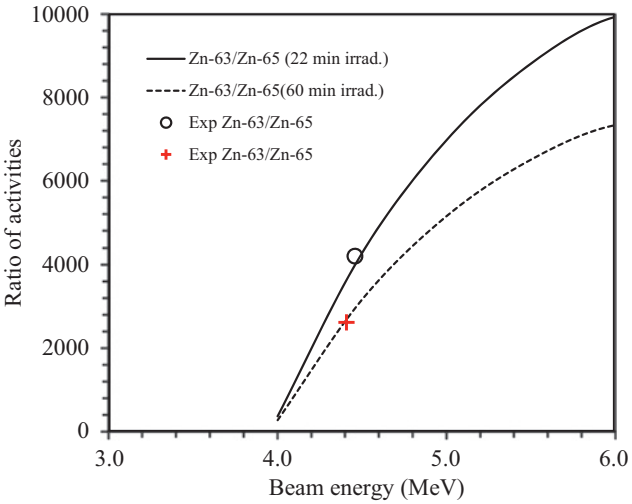

Figure 2: Ratios of normalised activities at EOB of the products formed in the irradiation of ^{nat}Cu with protons; *curves*: calculated from the standardised excitation functions given in Reference [33] – solid line for 22 min irradiation and dotted line for 60 min irradiation; *data points*: measured ratios – round symbol for 22 min irradiation and plus symbol for 60 min irradiation. The average proton energies in the irradiated foils were deduced as 4.46 ± 0.5 MeV and 4.41 ± 0.2 MeV, respectively, while using a primary proton energy of 5.02 MeV and 4.62 MeV (given by the accelerator parameters), respectively.

agreed with that obtained through the accelerator parameters, though the uncertainty of the activation method is high due to very low cross sections of the two products at energies < 6 MeV. Accelerator energy of 4.62 MeV and foil energy of 4.41 ± 0.2 MeV are in excellent agreement, but about 10% deviation was found between 5.02 MeV accelerator energy and 4.46 ± 0.5 MeV foil energy. The main reason was the use of foils of different thicknesses. For 4.62 MeV irradiation a thin foil was used and for the 5.02 MeV irradiation a thicker foil.

2.1.3 Proton flux measurement

The proton beam flux was measured by charge integration before reaching the target. The beam flux effective in the target was determined using the ^{nat}Cu(p, x)^{65}Zn monitor reaction induced in the mounted Cu-foil. The two flux values agreed within 6%.

2.1.4 Stack irradiation

For cross section measurements of proton induced reactions on ^{nat}Ni below 6 MeV, three stacks of foils were prepared. Each stack consisted of several 10 μm thick Ni foils (Goodfellow: purity 99.95%) with one (10 or 25 μm thick) Cu foil (Goodfellow: purity > 99%) placed in front to monitor the proton flux. The primary energy of protons falling on each stack was 5.02 MeV. The duration of irradiation was between 20 and 60 min. The beam energy degradation along the stack was calculated using the computer program based on the energy-range relation described by Williamson et al. [34].

2.2 Measurements at BC 1710

For studying proton induced reactions in the higher energy range up to 16 MeV, irradiations were carried out at the Baby Cyclotron (BC1710) of the Forschungszentrum Jülich, Germany. A newly developed target system and the quality of the available beam have been recently described [35]. For measurements on ^{nat}Ni, two stacks were irradiated. Each stack consisted of about 15 Ni foils of different thicknesses, with a few Cu foils (as monitors) and a few Al foils (as absorbers) interspersed in between. The duration of each irradiation was 10 min and the proton beam current was about 1 μA. It was determined exactly via the above

Table 1: Decay properties of the investigated radionuclides[a] formed in the interactions of ^{nat}Ni with protons of energy < 16 MeV.

Radionuclide	Half-life	E_γ (keV)	I_γ (%)	Reaction	Q-value (MeV)	Threshold energy (MeV)
^{60}Cu	23.7 min	826.4	21.7	^{61}Ni(p, 2n)^{60}Cu	−14.7	14.9
		1332.5	88.0	^{60}Ni(p, n)^{60}Cu	−6.9	7.0
^{61}Cu	3.33 h	282.9	12.2	^{62}Ni(p, 2n)^{61}Cu	−13.6	13.8
		656.0	10.8	^{61}Ni(p, n)^{61}Cu	−3.0	3.1
				^{60}Ni(p, γ)^{61}Cu	4.8	0.0
^{64}Cu	12.7 h	1345.8	0.54[b]	^{64}Ni(p, n)^{64}Cu	−2.4	2.5
^{55}Co	17.5 h	931.3	75.0	^{58}Ni(p, α)^{55}Co	−1.3	1.3
		477.2	20.2			
^{57}Co	271.8 d	122.1	85.6	^{58}Ni(p, 2p)^{57}Co	−8.2	8.3
				^{58}Ni(p, pn)^{57}Ni → ^{57}Co	−12.2	12.3
				^{60}Ni(p, α)^{57}Co	−0.3	0.3
^{58}Co	70.9 d	810.8	99.0	^{61}Ni(p, α)^{58}Co	−0.5	0.7
				^{62}Ni(p, αn)^{58}Co	−10.1	10.3
^{57}Ni	35.6 h	127.2	16.7	^{58}Ni(p, pn)^{57}Ni	−12.2	12.4
		1377.6	81.7			

[a] Taken from Reference [39].
[b] Taken from Reference [40].

mentioned monitor reactions. The primary energy of the protons incident on the first Cu foil was determined from a ratio of the ^{62}Zn/^{65}Zn activities [4, 32]. The beam energy degradation along the stack was calculated using the computer program STACK as mentioned above. The excitation functions of the monitor reactions were measured to check the beam parameters along the stack.

2.3 Measurement of radioactivity

The radioactivity of a reaction product in the activated foil was measured nondestructively using HPGe detector γ-ray spectrometry. The details on detectors and data analysis programs have already been reported [36–38]. Particularly, the activity measurement of the short-lived ^{60}Cu ($T_{1/2}$ = 23.7 min) was started about 40 min after the end of irradiation. All samples irradiated at BC 1710 were counted at a distance of 50 cm from the detector surface to keep the dead time below 5%. Each sample was recounted 2–3 times by giving sufficient cooling interval to check the half-lives of the activation products as well as to avoid disturbance by overlapping γ-lines from undesired products. After the decay of the short-lived radionuclides, the ^{61}Cu ($T_{1/2}$ = 3.4 h) activity was measured at sample-detector distances of 10 and 20 cm. The ^{57}Co and ^{58}Co activities were measured after proper cooling time to allow complete decay of short-lived precursor or the isomeric state. The radioactivity involved in samples irradiated at tandem accelerator was weak. Measurements were therefore done at a distance of 5 cm.

The efficiency versus energy curve of the HPGe gamma-ray detector was determined using the standard point sources ^{57}Co, ^{60}Co, ^{133}Ba, ^{137}Cs and ^{152}Eu traceable to PTB Braunschweig. The decay data of the investigated radionuclides were generally taken from the LUND/LBNL database [39] and are given in Table 1. Only in the case of ^{64}Cu the intensity of the weak 1345.8 keV γ-ray was taken from Reference [40].

2.4 Calculation of cross section

The count rate of each product radionuclide was extrapolated to the end of bombardment (EOB) and it was converted to decay rate by applying the usual corrections, like the intensity of the γ-ray used, the efficiency of the detector, etc. From the decay rate and proton flux determined via monitor reaction, the radionuclide production cross section was calculated using the well-known activation equation. The overall uncertainty in the cross section was obtained by a quadratic summing of the individual uncertainties involved in all parameters needed to calculate the cross section. The sources of uncertainties are given in Table 2. In general, the overall uncertainties associated in measured cross sections are between 7 and 15%.

Table 2: Sources of uncertainties in the measured cross sections.

Source of uncertainty	Uncertainties (%) in measurements using	
	Tandem Accelerator	BC 1710
Number of target nuclei	< 1	< 1
Counting statistics	0.2–10	0.7–9
Spectrum analysis	0.5	0.5
Efficiency of detector	4	4
Half-life of product	0.1–1.6	0.1–1.6
γ-ray intensity	0.2–6	0.2–6
Coincidence loss	< 0.5	< 0.5
Monitor cross section	8	6
Total	7–15	7–13

3 Results and discussion

The nuclear reaction cross section data measured in this work are summarized in Tables 3 and 4, listing the results of measurements done at the tandem accelerator and the BC 1710 cyclotron, respectively. The estimated uncertainties in the effective proton energies and the measured cross sections are also given. A detailed discussion on the formation of each investigated radionuclide is given in the following sections.

Table 3: Measured production cross sections of the radionuclides ^{61}Cu and ^{64}Cu in proton irradiation of Ni-nat using the 3 MV Tandem Accelerator.

Proton energy[a] (MeV)	Cross section (mb)	
	^{61}Cu	^{64}Cu[b]
3.96 ± 0.26	0.43 ± 0.03	105 ± 11
3.63 ± 0.29	0.36 ± 0.03	80 ± 9
3.42 ± 0.29	0.38 ± 0.03	48 ± 6
3.03 ± 0.30	0.23 ± 0.02	41 ± 5
2.82 ± 0.30	0.12 ± 0.01	23 ± 3
2.56 ± 0.30	0.07 ± 0.01	
2.37 ± 0.39	0.05 ± 0.01	
2.14 ± 0.39	0.04 ± 0.005	
1.85 ± 0.50	0.02 ± 0.003	
1.66 ± 0.50	0.009 ± 0.001	
1.49 ± 0.50	0.005 ± 0.001	

[a] The Tandem delivers proton with energy uncertainty of < 0.5%. The deviation given here describes the energy spread within each foil.
[b] Data normalized to 100% enrichment of ^{64}Ni.

3.1 ^{64}Ni(p,n)^{64}Cu reaction: Validation of experimental techniques

This reaction was investigated to validate our results, i.e. to demonstrate that the projectile energies and fluxes were accurately determined and the radioactivity of the product was properly assayed. We chose this reaction because of two reasons:

a) The target nuclide ^{64}Ni is the heaviest of all the stable Ni isotopes so that the product of the (p, n) reaction, i.e. ^{64}Cu, cannot be formed from any other target isotope. Although ^{64}Ni in ^{nat}Ni is only 0.926% (see above), the result can be unambiguously extrapolated to 100% enrichment.
b) This reaction has been thoroughly investigated by a large number of groups [1, 3, 5, 6, 10, 19–27] and a very critical standardization and evaluation of all the data has been performed [16].

A comparison of our experimental values with the recommended values should therefore vividly reveal the degree of agreement or deviation. All the literature data, normalized to γ-ray intensities in Table 1 and to 100% enrichment of ^{64}Ni, are shown in Figure 3 together with the evaluated and recommended curve by Aslam et al. [16]. The data obtained in the present work are also given. The agreement between our data and the evaluated curve over the whole investigated energy range is quite good. With regard to work done at the BC 1710, the authenticity of the measured data was already demonstrated (cf. [41]) and the present results confirm it. To show the reliability of the present measurements done at the tandem accelerator, we plot our data below 6 MeV (obtained both at tandem and BC 1710) on an expanded scale in Figure 4 together with the evaluated curve [16] and the more recent data by Adam Rebels et al. [10]. The results from the TENDL-2014 library [42] are also shown. An excellent agreement between our tandem data and the evaluated curve gives high confidence to our measurements; it demonstrates that the various techniques used in the determination of the experimental data at the tandem accelerator are reliable. The results also show that the agreement between the experiment and the global calculation reported in TENDL-2014 is not very satisfactory. A more rigorous calculation involving some target nucleus-specific parametrization, such as the one done in Reference [16], gives better agreement.

3.2 ^{nat}Ni(p,x)^{60}Cu reaction

The radionuclide ^{60}Cu can be produced via the reaction channels ^{60}Ni(p, n)^{60}Cu (E_{thr} = 7.0 MeV) and ^{61}Ni(p, 2n)^{60}Cu (E_{thr} = 14.9 MeV). Special care was necessary in the measurement of the short-lived ^{60}Cu ($T_{1/2}$ = 23.7 min) because of the high level of radioactivity. It was performed at 50 cm from the detector surface to

Table 4: Measured production cross sections of the radionuclides ^{60,61,64}Cu, ^{55,57,58}Co and ^{57}Ni in proton irradiation of Ni-nat using the Cyclotron BC 1710.

Proton energy (MeV)	Cross section (mb)						
	^{60}Cu	^{61}Cu	^{64}Cu[a)]	^{55}Co	^{57}Co	^{58}Co	^{57}Ni
15.9 ± 0.2	44.3 ± 3.3	5.05 ± 0.36		23.7 ± 1.7	234 ± 17	0.91 ± 0.07	24.6 ± 1.7
15.7 ± 0.2	46.7 ± 3.2	5.09 ± 0.36		24.1 ± 1.7	222 ± 16	0.80 ± 0.06	20.0 ± 1.4
15.5 ± 0.2	48.2 ± 3.5	4.07 ± 0.29	199 ± 20	23.5 ± 1.6	202 ± 15	0.99 ± 0.08	17.3 ± 1.2
14.9 ± 0.2	58.8 ± 4.1	3.69 ± 0.26	215 ± 21	22.7 ± 1.6	158 ± 11	0.88 ± 0.07	9.3 ± 0.7
14.2 ± 0.2	68.4 ± 4.8	2.76 ± 0.2		21.3 ± 1.5	110 ± 8	0.98 ± 0.08	4.4 ± 0.4
13.7 ± 0.3	74.4 ± 5.2	2.36 ± 0.17	353 ± 35	18.5 ± 1.3	76 ± 6	0.99 ± 0.08	2.4 ± 0.3
13.1 ± 0.3	78.8 ± 5.4	3.09 ± 0.22	439 ± 44	16.1 ± 1.1	42 ± 3	0.92 ± 0.07	
12.2 ± 0.3	75.3 ± 5.2	3.78 ± 0.27	538 ± 54	15.9 ± 1.1	21.2 ± 1.5	0.84 ± 0.07	
11.7 ± 0.3	73.3 ± 5.0	4.19 ± 0.29	558 ± 56	14.3 ± 1.0	14.6 ± 1.1	0.84 ± 0.07	
11.1 ± 0.3	73.8 ± 5.0	5.64 ± 0.41	649 ± 65	12.0 ± 0.8	11.7 ± 0.8	0.82 ± 0.06	
10.0 ± 0.3	79.8 ± 8.4	5.21 ± 0.37	707 ± 71	10.4 ± 0.7	9.6 ± 0.7	0.78 ± 0.06	
9.4 ± 0.4	66.3 ± 4.5	4.99 ± 0.35	690 ± 60	8.1 ± 0.6	7.5 ± 0.6	0.68 ± 0.05	
8.8 ± 0.4	58.4 ± 6.0	5.00 ± 0.35	597 ± 60	5.5 ± 0.4	5.2 ± 0.4	0.60 ± 0.05	
8.0 ± 0.4	41.5 ± 4.2	4.25 ± 0.35	576 ± 58	1.4 ± 0.2	2.6 ± 0.2	0.54 ± 0.04	
7.4 ± 0.4	18.1 ± 2.1	3.91 ± 0.40	527 ± 53	0.36 ± 0.05	1.7 ± 0.12	0.32 ± 0.03	
7.1 ± 0.4	6.7 ± 0.6	3.61 ± 0.30	457 ± 46	0.10 ± 0.02	0.37 ± 0.04	0.25 ± 0.03	
6.5 ± 0.4	0.32 ± 0.05	3.23 ± 0.28	427 ± 43		0.13 ± 0.02	0.22 ± 0.03	
6.2 ± 0.5		2.89 ± 0.25	342 ± 34			0.19 ± 0.03	
5.8 ± 0.5		2.51 ± 0.28	351 ± 35				
5.5 ± 0.5		2.27 ± 0.22	248 ± 25			0.17 ± 0.03	
5.0 ± 0.5		1.82 ± 0.19	243 ± 24			0.14 ± 0.03	
4.8 ± 0.5		1.69 ± 0.18	205 ± 20				
4.3 ± 0.3		1.16 ± 0.12	130 ± 13				
4.0 ± 0.3		0.91 ± 0.09	118 ± 12			0.12 ± 0.03	
3.6 ± 0.3		0.73 ± 0.08					
3.3 ± 0.3		0.48 ± 0.06					
3.1 ± 0.3		0.35 ± 0.05					
2.7 ± 0.3		0.14 ± 0.02					

[a)] Data normalized to 100% enrichment of ^{64}Ni.

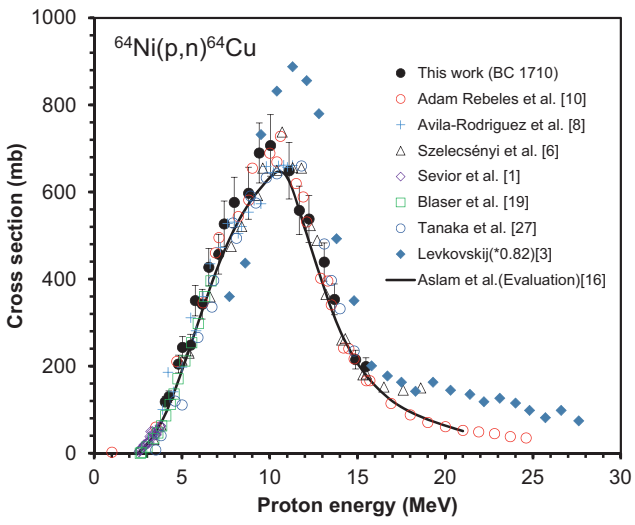

Figure 3: Excitation function of the ^{64}Ni(p, n)^{64}Cu reaction in comparison with former experimental results and evaluated values.

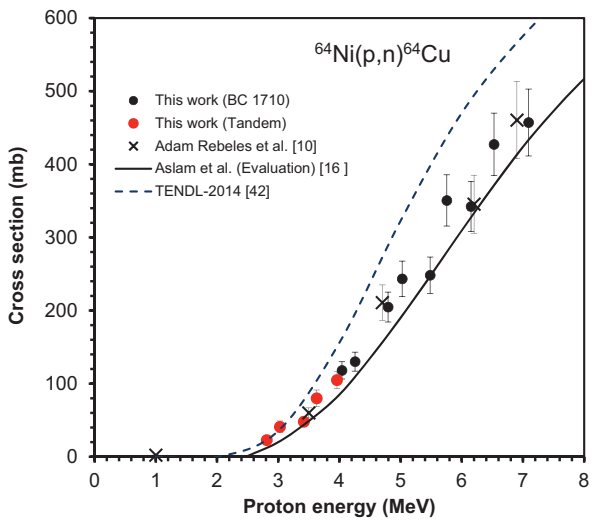

Figure 4: Excitation function of the ^{64}Ni(p, n)^{64}Cu reaction near its threshold region. The cross section value at the lowest energy given in Reference [10] is erroneous because it is below the threshold energy.

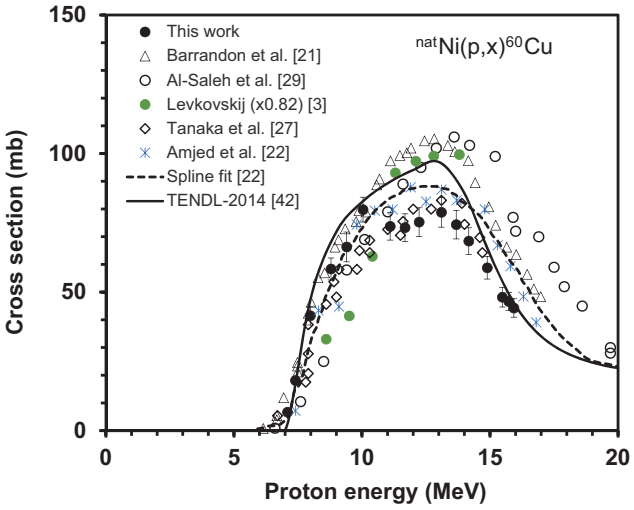

Figure 5: Excitation function of the $^{nat}Ni(p, x)^{60}Cu$ reaction in comparison with former results and TENDL-2014 library. The values by Levkovskij [3] and Tanaka et al. [27] were normalized to ^{nat}Ni.

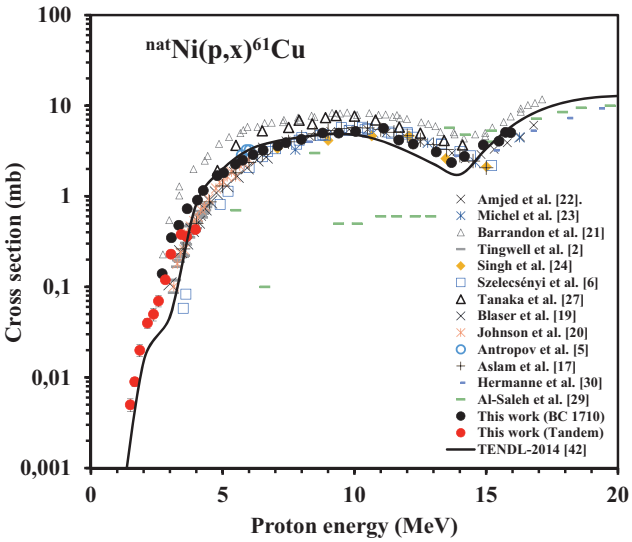

Figure 6: Excitation function of the $^{nat}Ni(p, x)^{61}Cu$ reaction in comparison with former results and TENDL-2014 library. The low-energy data (< 3 MeV) refer to the $^{60}Ni(p, \gamma)^{61}Cu$ reaction; they have been measured for the first time.

keep the dead time below 5% and to avoid the random sum-coincidence losses. The results are shown in Figure 5 together with the literature data. Whereas measurements by Barrandon et al. [21], Al-Saleh et al. [29] and Amjed et al. [22] were performed on ^{nat}Ni, the data reported by Tanaka et al. [27] and Levkovskij [3] referred to enriched ^{60}Ni. Due to the much higher abundance of ^{60}Ni in ^{nat}Ni as compared to that of ^{61}Ni and due to the much lower energy threshold of the $^{60}Ni(p, n)^{60}Cu$ reaction than that of the $^{61}Ni(p, 2n)^{60}Cu$ reaction, the major contribution to the formation of ^{60}Cu should originate from ^{60}Ni. We therefore normalized the data by Tanaka et al. [27] and Levkovskij [3] to ^{nat}Ni. Furthermore, the data by Levkovskij [3] were reduced as suggested by Takács et al. [43]. A factor of 0.82 was used as recommended by Qaim et al. [44] to normalize the monitor cross section used by Levkovskij. In Figure 5 the spline fitted curve [22] and the theoretical data from the TENDL-2014 library [42] are also shown. Our data agree with the spline fit.

3.3 $^{nat}Ni(p,x)^{61}Cu$ reaction

The radionuclide ^{61}Cu can be produced over the proton energy range up to 16.0 MeV by the reactions $^{60}Ni(p, \gamma)^{61}Cu$ ($E_{thr} = 0$), $^{61}Ni(p, n)^{61}Cu$ ($E_{thr} = 3.07$ MeV) and $^{62}Ni(p, 2n)^{61}Cu$ ($E_{thr} = 13.83$ MeV). The results obtained in this work are shown in Figure 6 together with earlier reported measurements and the results from TENDL-2014 library. A number of authors have reported data on this reaction [2, 5, 6, 17, 19–24, 27, 29, 30].

Since in the range from 3 MeV to 14 MeV the radionuclide ^{61}Cu would be mostly produced by the $^{61}Ni(p, n)^{61}Cu$ reaction, data for enriched ^{61}Ni are shown in Figure 6 after normalization to natural target. The first maximum in the excitation function around 8 MeV is attributed to the contribution of the $^{61}Ni(p, n)^{61}Cu$ reaction. Above 15 MeV, the cross section rises again due to the increasing contribution of the $^{62}Ni(p, 2n)^{61}Cu$ reaction. Below 3 MeV, there is no data available. Somehow that region was hitherto not explored by any group. Because ^{61}Cu is produced in that energy region only by the $^{60}Ni(p, \gamma)$ reaction, the measured cross section is rather low and a very careful experiment was necessary for this measurement by irradiation of samples at the tandem accelerator. These results are thus being reported for the first time.

3.4 $^{nat}Ni(p,x)^{55}Co$ reaction

Our results are shown in Figure 7 together with the literature values. Since the radionuclide ^{55}Co ($T_{1/2} = 17.53$ h) is produced in natural nickel up to a proton energy of about 20 MeV via a single reaction channel, namely $^{58}Ni(p, \alpha)^{55}Co$ ($E_{thr} = 1.4$ MeV), data measured on enriched ^{58}Ni [3, 9, 27] were normalized to ^{nat}Ni. The results obtained in this work are in good agreement with Amjed et al. [22], Khandaker et al. [26] and Hermanne et al. [30]. The data by Barrandon et al. [21] are low in the energy range of 12–18 MeV. The TENDL-2014 library data on the other hand are somewhat high in the peak region of

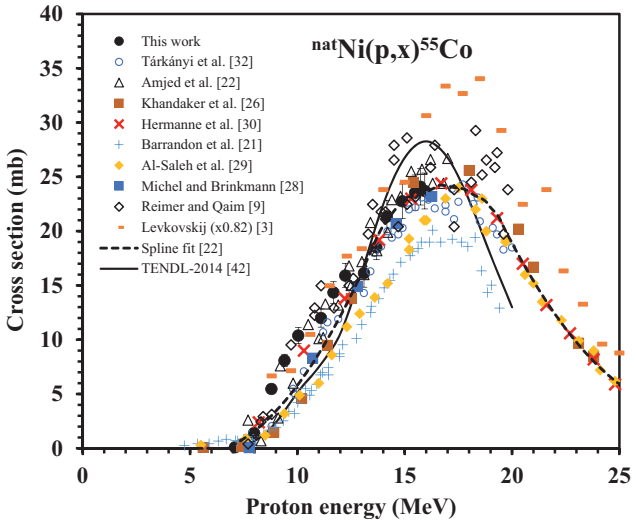

Figure 7: Excitation function of the ^{nat}Ni(p, x)^{55}Co reaction in comparison with former results and TENDL-2014 library. Our data are close to the spline fit given by Amjed et al. [22].

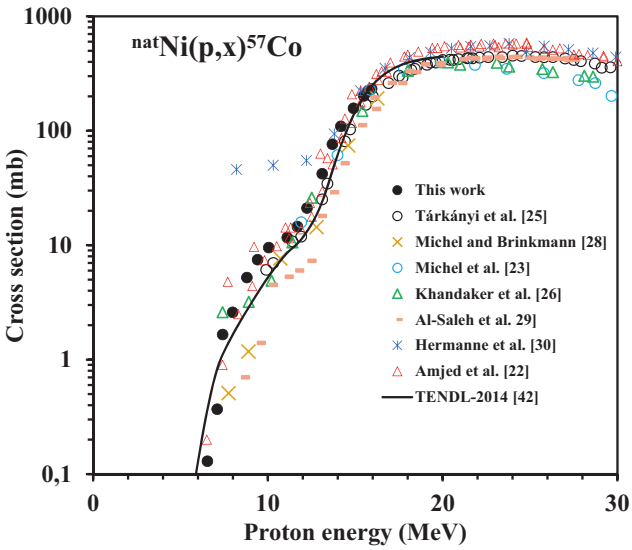

Figure 8: Excitation function of the ^{nat}Ni(p, x)^{57}Co reaction in comparison with former results and TENDL-2014 library.

the excitation function and show an energy shift of about 1.5 MeV in the rising part of the excitation curve. Our measured data agree well with the spline fit given by Amjed et al. [22].

3.5 ^{nat}Ni(p,x)^{57}Co reaction

The excitation function for the formation of ^{57}Co in the interaction of protons with nickel of natural isotopic composition is shown in Figure 8. The available literature values [22, 23, 25, 26, 28–30] are also given. The radionuclide ^{57}Co is produced via the reaction channels ^{58}Ni(p, 2p)^{57}Co (E_{thr} = 8.3 MeV), ^{60}Ni(p, α)^{57}Co (E_{thr} = 0.3 MeV) and ^{58}Ni(p, pn)^{57}Ni → ^{57}Co (E_{thr} = 12.3 MeV). In the measurement of the ^{57}Co radioactivity, special attention was paid to complete decay of ^{57}Ni before counting. The results achieved in this work are in good agreement with those of Amjed et al. [22], Tárkányi et al. [25], Khandaker et al. [26] and Michel et al. [23, 28]. Below 10 MeV the data reported by Al-Saleh et al. [29] are shifted towards higher energy. The data obtained by using enriched ^{58}Ni [9] were normalized to ^{nat}Ni. Those data refer only to the contribution of the (p, 2p) reaction and are therefore not shown in Figure 8. From the shape of the excitation curve given in Figure 8 it is obvious that the low energy part up to 10 MeV is determined by the ^{60}Ni(p, α)^{57}Co reaction whereas beyond 10 MeV the other two processes contribute strongly. The TENDL-2014 data [42] reproduce the experimental curve quite well.

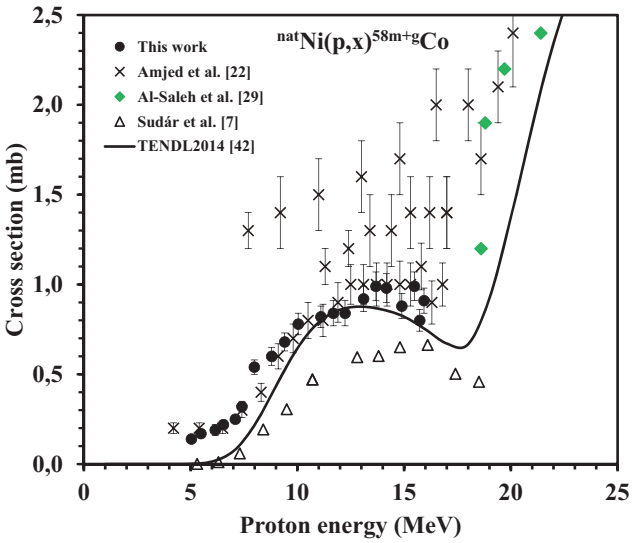

Figure 9: Excitation function of the ^{nat}Ni(p, x)$^{58m+g}$Co reaction in comparison with former results and TENDL-2014 library.

3.6 ^{nat}Ni(p,x)$^{58m+g}$Co reaction

The radionuclide ^{58}Co has two isomeric states, a long-lived ground state ^{58g}Co ($T_{1/2}$ = 70.82 d) and a metastable state ^{58m}Co ($T_{1/2}$ = 9.15 h). The metastable state decays completely to the ground state. Therefore, counting was performed after the complete decay of ^{58m}Co to the ground state and cumulative cross sections were determined. The excitation function for the formation of $^{58m+g}$Co is shown in Figure 9 together with the available literature values [7, 22, 29] which are rather discrepant in the low energy region. As shown in Figure 9, Amjed et al. [22] reported data

which can be categorized into three series. The series with the lowest values is consistent with our data but the other values appear to be overestimated and are not comparable to this work. Sudár et al. [7] reported ^{61}Ni(p, α)$^{58m+g}$Co reaction cross sections, based on measurements using highly enriched target material. Those data were converted to ^{nat}Ni. Considering the threshold energies of the two possible reactions contributing to the formation of $^{58m+g}$Co, viz. ^{61}Ni(p, α)^{58}Co and ^{62}Ni(p, αn)^{58}Co, it is obvious that the normalized values of Sudár et al. [7] are too low because they relate only to one reaction, i.e. the ^{61}Ni(p, α)^{58}Co. We interpret the rapid increase in the cross section beyond 16 MeV to be due to the increasing contribution of the ^{62}Ni(p, αn)^{58}Co process. The TENDL-2014 supports this rising trend, though there is some energy shift.

3.7 ^{nat}Ni(p,x)^{57}Ni reaction

Our results given for this reaction in Table 4 are very consistent with the standard data for this reaction published by the IAEA [34]. This fact confirms again that the experimental parameters, i.e., the detector efficiency curve, the beam current, the beam incident energy etc., used in the determination of cross section data at BC 1710 are reliable.

4 Conclusion

A new facility has been constructed at the 3 MV Tandem Accelerator at Savar in Bangladesh for measuring proton induced reaction cross sections near their thresholds, and the beam parameters have been characterized. The authenticity of the data obtained was established by comparison with the results for the well investigated reaction ^{64}Ni(p, n)^{64}Cu. Excitation functions of the proton induced nuclear reactions on nickel leading to the formation of several other nuclides were also measured from threshold to 16 MeV, using the Tandem Accelerator and the Cyclotron BC 1710 at Jülich, Germany. A few results are new, in particular the demonstration of the occurrence of the ^{60}Ni(p, γ)^{61}Cu reaction; the other data are of confirmatory nature and strengthen the database. Below 3 MeV, the data of the reaction ^{nat}Ni(p, x)^{61}Cu obtained in this work could be useful to monitor beam parameters of low energy accelerators.

Acknowledgement: Md. Shuza Uddin thanks the Alexander von Humboldt Foundation for supporting his follow-up visit in 2014 to the Forschungszentrum Jülich to do part of the present work there, and especially for financial support to conduct this research work at INST, Savar, Bangladesh. The authors thank the operational crews of the Baby Cyclotron BC 1710 of the Forschungszentrum Jülich and the 3 MV Tandem Accelerator of AERE, Savar, Bangladesh, for their help in performing the irradiations.

References

1. Sevior, M. E., Mitchell, L. W., Anderson, M. R., Tingwell, C. W.: Absolute cross sections of proton induced reactions on Cu-65, Ni-64, Cu-63. Australian Journal of Physics **36**, 463 (1983).
2. Tingwell, C. I. W., Hansper, V. Y., Tims, S. G., Scott, A. F.: Cross sections of proton induced reactions on ^{61}Ni. Nucl. Phys. A **480**, 162 (1988).
3. Levkovskij, V. N.: Activation cross sections of nuclides of average masses ($A = 40–100$) by protons and alpha-particles with average energies ($E = 10–50$ MeV), Inter-Vesi, Moscow (1991).
4. Piel, H., Qaim, S. M., Stöcklin, G.: Excitation functions of (p, xn) reactions on ^{nat}Ni and highly enriched ^{62}Ni: possibility of production of medically important radioisotope ^{62}Cu at a small cyclotron. Radiochim. Acta **57**, 1 (1992).
5. Antropov, A. E., Gusev, V. P., Zhuravlev, Yu. Yu., Zarubin, P. P., Kolozhvari, A. A., Smirnov, A. V.: Total cross sections of (p, n) reaction on the nuclei of isotopes nickel and zink at $E(p) = 5–6$ MeV. Izv. Rossiiskoi Akademii Nauk, Ser. Fiz. **56**, 198 (1992).
6. Szelecsényi, F., Blessing, G., Qaim, S. M.: Excitation functions of proton induced nuclear reaction on enriched ^{61}Ni and ^{64}Ni: possibility of production of no-carrier-added ^{61}Cu and ^{64}Cu at a small cyclotron. Appl. Radiat. Isot. **44**, 575 (1993).
7. Sudár, S. Szelecsényi, F., Qaim, S. M.: Excitation function and isomeric cross-section ratio for the ^{61}Ni(p, α)^{58m,g}Co process. Phys. Rev. **48**, 3115 (1993).
8. Avila-Rodriguez, M. A., Nye, J. A., Nickles, R. J.: Simultaneous production of high specific activity ^{64}Cu and ^{61}Co with 11.4 MeV protons on enriched ^{64}Ni nuclei. Appl. Radiat. Isot. **65**, 1115 (2007).
9. Reimer, P., Qaim, S. M.: Excitation functions of proton induced reactions on highly enriched ^{58}Ni with special relevance to the production of ^{55}Co and ^{57}Co. Radiochim. Acta **80**, 113 (1998).
10. Adam Rebeles, R., Van Den Winkel, P., Hermanne, A., Tárkányi, F.: New measurement and evaluation of the excitation function of ^{64}Ni(p,n) reaction for the production of ^{64}Cu. Nucl. Instrum. Meth. B **267**, 457 (2009).
11. Spellerberg, S., Reimer, P., Blessing, G., Coenen, H. H., Qaim, S. M.: Production of ^{55}Co and ^{57}Co via proton induced reactions on highly enriched ^{58}Ni. Appl. Radiat. Isot. **49** 1519 (1998).
12. McCarthy, D. W., Bass, L. A., Cutler, P. D., Shefer, R. E., Klinkowstein, R. E., Herrero, P., Lewis, J. S., Cutler, C. S., Anderson, C. J., Welch, M. J.: High purity production and potential applications of Copper-60 and Copper-61. Nucl. Med. Biol. **26**, 351 (1999).
13. McCarthy, D. W., Shefer, R. E., Klinkowstein, R. E., Bass, L. A., Margeneau, W. H., Cutler, C. S., Anderson, C. J., Welch, M. J.: Efficient production of high specific activity ^{64}Cu using a biomedical cyclotron. Nucl. Med. Biol. **24**, 35 (1997).

14. Szajek, L. P., Meyer, W., Plascjak, P., Eckelman, W. C.: Semiremote production of [^{64}Cu]$CuCl_2$ and preparation of high specific activity [^{64}Cu]Cu-ATSM for PET studies. Radiochim. Acta **93**, 239 (2005).
15. Sadeghi, M., Amiri, M., Roshanfarzad, P., Avila, M., Tenreiro, C.: Radiochemical studies relevant to the no-carrier added production of ^{61,64}Cu at a cyclotron. Radiochim. Acta **96**, 399 (2008).
16. Aslam, M. N., Sudár, S., Hussain, M., Malik, A. A., Shah, H. A., Qaim, S. M.: Charged particle induced reaction cross section data for production of the emerging medically important positron emitter ^{64}Cu: a comprehensive evaluation. Radiochim. Acta **97**, 669 (2009).
17. Aslam, M. N., Qaim, S. M.: Nuclear model analysis of excitation functions of proton, deuteron and α-particle induced reactions on nickel isotopes for production of the medically interesting copper-61. Appl. Radiat. Isot. **89,** 65 (2014).
18. Amjed, N., Hussain, M., Aslam, M. N., Tárkányi, F., Qaim, S. M.: Evaluation of nuclear reaction cross sections for optimization of production of the emerging diagnostic radionuclide ^{55}Co. Appl. Radiat. Isot., submitted.
19. Blaser, J. P., Boehm, F., Marmier, P., Scherrer, P.: Anregungsfunktionen und Wirkungsquerschnitte der (p, n)-Reaktion (II). Helvetica Physics Acta **24**, 441 (1951).
20. Johnson, C. H., Trail, C. C., Galonsky, A.: Thresholds for (p, n) reactions on 26 intermediate-weight nuclei. Phys. Rev. B **136**, 1719 (1964).
21. Barrandon, J. N., Debrun, J. L., Kohn, A., Spear, R. H.: A study of the main radioisotopes obtained by irradiation of Ti, V, Cr, Fe, Ni, Cu and Zn with protons from 0 to 20 MeV. Nuclear Instrum. Meth. **127**, 269 (1975).
22. Amjed, N., Tárkányi, F., Hermanne, A., Ditroi, F., Takacs, S., Hussain, M.: Activation cross-sections of proton induced reactions on natural Ni up to 65 MeV. Appl. Radiat. Isot. **92**, 73 (2014).
23. Michel, R., Weigel, H., Herr, W.: Proton-induced reactions on nickel with energies between 12 and 45 MeV. Zeitschrift fuer Physik A **286**, 393 (1978).
24. Singh, B. P., Sharma, M. K., Musthafa, M. M., Bhardwaj, H. D., Prasad, R.: A study of pre-equilibrium emission in some proton- and alpha-induced reactions. Nucl. Instrum. Meth. A **562**, 717 (2006).
25. Tárkányi, F., Szelecsényi, F., Kopecky, P.: Excitation functions of proton induced nuclear reactions on natural nickel for monitoring beam energy and intensity. Appl. Radiat. Isot. **42**, 513 (1991).
26. Khandaker, M. U., Lee, M. W., Kim, K. S., Kim, G. N.: Excitation functions of (p, x) reactions on natural nickel up to 40 MeV. Nucl. Instrum. Meth. B **269**, 1140 (2011).
27. Tanaka, S., Furukawa, M., Chiba, M.: Nuclear reactions of nickel with protons up to 56 MeV. J. Inorg. Nucl. Chem. **34**, 2419 (1972).
28. Michel, R., Brinkmann, G.: On the depth-dependent production of radionuclides ('A' between 44 and 59) by solar protons in extraterrestrial matter. J. Radioanal. Chem. **59**, 467 (1980).
29. Al-Saleh, F. S., Al-Mugren, K. S., Azzam, A.: Excitation functions of (p, x) reactions on natural nickel between proton energies of 2.7 and 27.5 MeV. Appl. Radiat. Isot. **65**, 104 (2007).
30. Hermanne, A., Adam Rebeles, R., Tárkányi, F., Takács, S.: Excitation functions of proton induced reactions on ^{nat}Os up to 65 MeV: experiments and comparison with results from theoretical codes. Nucl. Instrum. Meth. B **345**, 58 (2015).
31. Uddin, M. S., Borua, B. S., Shariff, M. A., Hasan, M. M., Rashid, M. A., Kamal, M.: Investigation of elemental and radiological contamination of soils in two shipyards in Chittagong, Bangladesh. Radiochim. Acta **102**, 741 (2014).
32. Tárkányi, F., Szelecsényi, F., Takács, S.: Determination of effective bombarding energies and flux using improved stacked-foil technique. Acta Radiol. Suppl. **376**, 72 (1991) (Abstract).
33. Tárkányi, F., Gul, K., Hermanne, A., Mustafa, M. G., Nortier, F. M., Qaim, S. M., Scholten, B., Shubin, Yu, Takács, S., Zhuang, Y.: Beam monitor reactions: in charged particle cross section database for medical radioisotope production. IAEA-TECDOC-1211, pp. 49–152 (2001).
34. Williamson, C. F., Boujot, J. P., Picard, J.: Tables of range and stopping power of chemical elements for charged particles of energies from 0.5 to 500 MeV. Report CEA-R 3042 (1966).
35. Spellerberg, S., Scholten, B., Spahn, I., Bolten, W., Holzgreve, M., Coenen, H. H., Qaim, S. M.: Target development for diversified irradiations at a medical cyclotron. Appl. Radiat. Isot. **104**, 106 (2015).
36. Sudár, S., Qaim, S. M.: Excitation functions of proton and deuteron induced reactions on iron and alpha-particle induced reactions on manganese in the energy region up to 25 MeV. Phys. Rev. C **50**, 2408 (1994).
37. Uddin, M. S., Zaman, M. R., Hossain, S. M., Spahn, I., Sudár, S., Qaim, S. M. : An Am/Be neutron source and its use in integral tests of differential neutron reaction cross section data. Appl. Radiat. Isot. **68**, 1656 (2010).
38. Uddin, M. S., Scholten, B., Hermanne, A., Sudár, S., Coenen, H. H., Qaim, S. M.: Radiochemical determination of cross sections of α-particle induced reactions on ^{192}Os for the production of the therapeutic radionuclide ^{193m}Pt. Appl. Radiat. Isot. **68**, 2001 (2010).
39. Chu, S. Y. F., Ekström, L. F., Firestone, R. B.: Lund/LBNL Nuclear Data Service, Version 2. http://nucleardata.nuclear.lu.se/nucleardata/toi/ (1999).
40. Qaim, S. M., Bisinger, T., Hilgers, K., Nayak, D., Coenen, H. H.: Positron emission intensities in the decay of ^{64}Cu, ^{76}Br and ^{124}I. Radiochim. Acta **95**, 67 (2007).
41. Buchholz, M., Spahn, I., Scholten, B., Coenen, H. H.: Cross section measurements for the formation of ^{52}Mn and its isolation with a non-hazardous element. Radiochim. Acta **101**, 491 (2013).
42. Koning, A. J., Rochman, D., van der Marck, S. C., Kopecky, J., Sublet, J. Ch., Pomp, S., Sjostrand, H., Forrest, R., Bauge, E., Henriksson, H., Cabellos, O., Goriely, S., Leppanen, I., Leeb, H., Plompen, A., Mills, R.: TENDL-2014: TALYS-based evaluated nuclear data library, 11 December 2014.
43. Takács, S., Tárkányi, F., Sonck, M., Hermanne, A.: Investigation of the ^{nat}Mo(p, x)^{96m,g}Tc nuclear reaction to monitor proton beams: new measurements and consequences on the earlier reported data. Nucl. Instrum. Meth. B **198**, 183 (2002).
44. Qaim, S. M., Sudár, S., Scholten, B., Koning, A. J., Coenen, H. H.: Evaluation of excitation functions of ^{100}Mo(p, d + pn)^{99}Mo and ^{100}Mo(p, 2n)^{99m}Tc reactions: estimation of long-lived Tc-impurity and its implication on the specific activity of cyclotron-produced ^{99m}Tc. Appl. Radiat. Isot. **85**, 101 (2014).